High-energy hadron-nucleus collisions*

G. Bialkowski

Institute for Theoretical Physics, University of Warsaw, Warsaw, Poland

C. B. Chiu† and D. M. Tow†

Center for Particle Theory, University of Texas, Austin, Texas 78712

(Received 23 December 1976)

A new space-time model for hadron-nucleus collision is proposed, in which produced particles at the instant of creation not only are immature, but their maturity rate is enhanced in the presence of other hadronic matter, as in a nucleus. The model's only free parameter, describing the maturity enhancement, is fixed by normalizing to the 200-GeV p-A multiplicity data at a fixed A. The parameter-free model then predicts correctly the p-A differential multiplicity as function of the pseudorapidity η and A, the multiplicity energy dependence, the π-A differential multiplicity, and the A dependences of $\sigma_{\mathrm{inel}}^{pA}$ of $\sigma_{\mathrm{inel}}^{\pi A}$. We also show quantitatively that the so-called cut-type model and fan-plus-cut-type model do not agree with the data.

I. INTRODUCTION

Because of the possibility of extracting out infomation about the space-time development of hadron-hadron (h-h) collisions, high-energy hadron-nucleus (h-A) collisions in the last few years have become a very active area of research, both experimentally[1,2] and theoretically.[3,4] The two most outstanding experimental characteristics are (1) the relatively slow rate of increase in the charged-multiplicity ratio $R_A = \langle n_A \rangle / \langle n_N \rangle$ as a function of A, and (2) for large pseudorapidity η, the differential multiplicity ratio $dR_A/d\eta = (dn_A/d\eta)/(dn_N/d\eta)$ is essentially 1 for all A. These properties imply that certain degrees of freedom are frozen and that the additional multiplicity does not come from the large-η region. Several qualitative methods have been proposed to freeze certain degrees of freedom. Various authors[5-9] have considered the possibility that it takes a certain time τ_0, of the order of $1/m_\pi$ in the rest frame of the incident particle, to develop small-momentum partons which can then interact with the at-rest nucleon (or nucleus). In the laboratory frame (or nucleus rest frame), Lorentz dilation then causes the large-rapidity particles to take a long time to develop small-momentum partons, so that they will be spatially separated from succeeding nucleons in the nucleus and therefore will not interact with them. This proposal freezes some of the degrees of freedom, and the larger the rapidity of the particle the larger the probability for it to be frozen. However, as we will show in Sec. III, our quantitative calculations show that this model, even in its most general form with two free parameters, does not agree with the data,[2] because unless $\tau_0 \ll 1/m_\pi$, the larger-rapidity particles are frozen too much so that the peaks are too far to the left of the experimental peaks and there are too few

particles to the right of the peaks. Other authors did not input this temporal freezing of degrees of freedom and have considered a leading-particle cascade (or cut-type) model.[4,10] The authors of Ref. 10 argued that, due to the weak triple-Pomeron coupling, produced secondaries do not participate in the cascade process (i.e., the fan contribution is negligible) and that property (2) is purely a kinematic energy-momentum-conservation effect on the leading-particle cascade alone. Again, in Sec. III our quantitative calculation show that this model, with one free parameter, also does not agree with the data, because the cut contribution creates many large-rapidity particles and, if we assume that all the particles are coming solely from this contribution, then the peak in $dn_A/d\eta$ does not shift enough to the left as A increases.

In this paper we propose a new space-time description of high-energy hadron-nucleus collisions.[11] We suggest that immediately after a collision, the outgoing particles are "immature" (or "bare"); i.e., if they undergo a collision with another particle right at that moment, they have a very small inelastic cross section. There is a typical maturity time, of the order of $1/m_\pi$ in the rest frame of the particle, after which its inelastic cross section is the same as a bona fide physical particle. This is similar in spirit to the temporal freezing of degrees of freedom of Refs. 5-9. However, we also propose that in the presence of other hadronic matter, as in a nucleus, the maturity time is shortened by an amount which is proportional to the amount of hadronic matter traversed. Our physical picture is that immediately after a collision, immature or bare particles are produced; if given enough time, these bare particles will then dress themselves up with gluons (or meson clouds) to become physical particles; the pres-

ence of other hadronic matter expedites the dressing of these bare particles with gluons to become physical particles. Our model is therefore a modified cascade model, modified in the sense that as the result of the immaturity effect the effective internal (corresponding to subsequent collisions in the nucleus) inelastic couplings are always smaller than the external ones. Furthermore, once the external inelastic couplings are given, the internal inelastic couplings depend on only one free parameter, the one that governs the maturity rate due to the traversal through other hadronic matter.

In the next section, we make quantitative this maturity idea and formulate our model to calculate $dn_A^p/d\eta$, $R_A^p(E_L)$, $dn_A^\pi/d\eta$, σ_{inel}^{pA}, and $\sigma_{inel}^{\pi A}$, where the superscripts p and π denote the incident hadron. Section III shows that our model predictions are all in agreement with the data. On the other hand, it also shows that the models of Refs. 5-10 do not agree with the data. Section IV ends with a summary.

II. FORMULATION OF MODEL

We first discuss what is the average number of nucleons $\bar{K}$ that an incident hadron encounters as it traverses through a given nucleus with A nucleons. We assume the nucleus is a sphere of radius r_A with uniform density ρ. First consider the case where the hadron is incident on the center of the nucleus, i.e., at zero impact parameter. Let K be the number of nucleons within a cylinder of length $2r_A$ and width $2r_N$, where r_N is the radius of a nucleon. We know

$$A = \rho(\tfrac{4}{3}\pi r_A^3)$$

$$= \frac{K}{\pi r_N^2(2r_A)}(\tfrac{4}{3}\pi r_A^3)$$

$$= \frac{2K}{3}\left(\frac{r_A}{r_N}\right)^2 ;$$

this implies

$$K = \frac{3A}{2}\left(\frac{r_N}{r_A}\right)^2 . \tag{1}$$

We obtain $\bar{K}$ by averaging over impact parameter; this gives

$$\bar{K} = A\left(\frac{r_N}{r_A}\right)^2 . \tag{2}$$

Since $r_A \approx 1.1\, r_N A^{1/3}$ (Ref. 12), we get

$$\bar{K} \approx 0.8\, A^{1/3} , \tag{3}$$

which is expected to be correct only for large A.

Unlike many others, we do not use the variable $\bar{\nu}_h \equiv A\sigma_{inel}^{hN}/\sigma_{inel}^{hA}$ as a measure of the apparent thick-

TABLE I. Relationship between A, $\bar{\nu}_p$, $\bar{\nu}_\pi$, and $\bar{K}$.

A	$\bar{\nu}_p$	$\bar{\nu}_\pi$	$\bar{K}$
30	2.00	1.74	2.5
60 (emulsion)	2.50	2.07	3.1
108	3.00	2.40	3.8
282 (extrapolated)	4.00	3.05	5.2

ness of the nucleus, because the interpretation of $\bar{\nu}_h$ as the average number of inelastic collisions that the incident particle encounters in traversing the nucleus is model-dependent, especially in view of the presence of the immaturity effect. In comparing our model predictions with the data of Ref. 2, which are presented in terms of $\bar{\nu}_h$, we use $\bar{\nu}_h$ only to tell us the value of A and then use Eq. (3) to calculate $\bar{K}$. The relationship of A, $\bar{\nu}_p$, $\bar{\nu}_\pi$, and $\bar{K}$ is tabulated in Table I. Notice that $\bar{K}$ is independent of the type of incident particle. Later we will explain what gives rise to the difference between p-A and π-A collisions.

Given a nucleus A, we want to find the multiplicity rapidity distribution as the result of the incident particle (and subsequently also the produced secondaries) colliding with $\bar{K}$ nucleons. Various phenomenological analyses indicate that meson clusters are predominantly the directly produced objects in high-energy multiparticle production. For definiteness we assume that these clusters decay asymptotically to an average of three pions. Our conclusions are insensitive to the exact value chosen for this number. The cluster rapidity distribution may be assumed to be similar in shape to the observed pion rapidity distribution.[13] The fact that it is clusters which are produced and which initiate subsequent collisions already reduces the total number of degrees of freedom.

We formulate our problem in terms of the rapidity variable y. At the end of our calculation we kinematically transform our y distributions into pseudorapidity η distributions with the relation

$$\eta = \sinh^{-1}\left(\frac{m_T}{p_T}\sinh y\right), \tag{5}$$

where $m_T \equiv (m_\pi^2 + p_T^2)^{1/2}$ with the nominal value of $p_T = 0.35$ GeV/c. We divide the rapidity into uniform intervals of length Δ and write

$$y_i = i\Delta, \quad i = 1, 2, \ldots, I. \tag{6}$$

At 200 GeV, the rapidity of the incident proton is $y^p = 6.1$; in our calculation we set $y_{max} = 7.0$ to effectively take into account that kinematically y^π can be larger than y^p by as much as 1.9. In our

calculation we set $\Delta = 0.5$. We have also repeated our calculation with $\Delta = 0.25$ and found that our results are completely insensitive to the choice of Δ.

We first consider p-A collision. We denote the nucleon and meson-cluster rapidity distributions after the first collision by $N_1(i)$ and $M_1(i)$. If we denote the probability that the incident proton when encountering a nucleon would undergo an inelastic collision by P_N, then $N_1(i)$ and $M_1(i)$ are given by

$$N_1(i) = P_N V_N(i,I) + \frac{1 - P_N}{\Delta} \delta_{iI} , \qquad (7a)$$

$$M_1(i) = P_N V_M(i,I) , \qquad (7b)$$

where $V_N(i,I)$ and $V_M(i,I)$ are, respectively, the nucleon and meson-cluster rapidity distributions normalized to inelastic events. The latter are known from p-N data. From the 200-GeV p-N data of Ref. 2 we can parameterize $V_m(i,I)$ as

$$V_M(i,I) = \begin{cases} C_0(1 - e^{-y_i})^2 & \text{for } y_i \leq y_I/2 \quad (8a) \\ C_0(1 - e^{-(y_I - y_i)})^2 & \text{for } y_i \geq y_I/2 , \quad (8b) \end{cases}$$

where $C_0 = 1.87$.[14] Since we know the leading nucleon has an elasticity $\xi \approx 0.5$ (for the inelastic events), after taking into account both the outgoing projectile nucleon and the recoil nucleon, one parameterization for $V_N(i,I)$ is just

$$V_N(i,I) = V_N^R(i,I) + V_N^L(i,I)$$
$$= \delta_{i,I'} + \delta_{i,I''} , \qquad (9a)$$

where $y_{I'} = y_I + \ln\xi$ and $y_{I''} = -\ln\xi$. We can get another parameterization for $V_N(i,I)$ by noticing that the outgoing projectile nucleon has an approximate flat distribution as a function of the center-of-mass longitudinal momentum p_z^*, i.e., $dn/dp_z^* \approx C$.[15] Using the constraint

$$\xi = \int_0^1 \frac{dn}{dx} x \, dx ,$$

where $x = 2p_z^*/\sqrt{s}$, we can derive

$$\frac{dn}{dy} \approx 4\xi e^{-y_{\max}/2} \cosh(y - y_{\max}/2) ,$$

resulting in a second parameterization for $V_N(i,I)$ as

$$V_N(i,I) = 4\xi e^{-y_I/2} [\sinh(y_i - y_I/2)$$
$$- \sinh(y_i - \Delta - y_I/2)] , \qquad (9b)$$

where now V_N^R and V_N^L are just, respectively, the right half and the left half of V_N. We found that parameterizations (9a) and (9b) give rise to no significant difference for the calculation of the final meson distribution.

Now we come to the probability of inelastic collision P_N, which can also be estimated from h-h collision data. We make use of the usual disk approximation. Here the scattering amplitude is assumed to be purely imaginary and to be constant within a disk of radius r. Then the S matrix at impact parameter b is given by

$$S(b) = S\theta(r - b) ,$$

where $0 \leq S \leq 1$, with $S = 0$ corresponding to the limit of a black disk and $S = 1$ corresponding to the absence of interaction. The inelastic-collision probability for $b \leq r$ is given by

$$P_N = 1 - S^2 , \qquad (10)$$

and the complementary (or noninelastic) probability $1 - P_N = S^2$ represents the square of the amplitude for the coherent superposition of the elastic scattering and through-going waves.[16] Within the disk approximation S is readily obtained through the experimental ratio of inelastic to total cross sections. In particular,

$$\frac{\sigma_{inel}}{\sigma_{tot}} = \frac{1 - S^2}{2(1 - S)} = \frac{1 + S}{2} . \qquad (11)$$

We use the nominal values of $\sigma_{inel} = 32$ mb and $\sigma_{tot} = 40$ mb for pp collisions and get

$$P_N = 0.64 . \qquad (12a)$$

Similarly, for π^--induced reactions, using $\sigma_{inel} = 21$ mb and $\sigma_{tot} = 24$ mb,[17] we get

$$P_\pi = 0.44 . \qquad (12b)$$

Equations (7), (8), (9), and (12) completely specify the rapidity distributions after the first collision. To be able to discuss subsequent collisions, we must first formulate the immaturity effect. As mentioned in the Introduction, particles immediately after a collision are assumed to be immature, i.e., they have zero inelastic-collision probability. They gradually acquire a maturity status through both a "spontaneous maturity process" and an "induced maturity process" owing to the presence of other hadronic matter. We denote the immature probability by Q, and assume that Q falls off exponentially with time t and with the amount of hadronic matter traversed. The amount of hadronic matter traversed between successive collisions is just the internucleon distance within the nucleus, which we denote by d; the value of d is given by $d = 2r_A/K = 1.3/m_\pi$, where we have made use of Eq. (1) together with the numerical values quoted in Ref. 12. The immaturity probability for a particle with velocity $\beta = v/c$ or $\cosh y = \gamma = (1 - \beta^2)^{-1/2}$ at the mean distance d away or at time $t = d/v$ after its creation is given by

$$Q(y) = e^{-tv/\tau_0 \, \gamma v} \, e^{-d/z_0}$$

$$= e^{-d/\tau_0 \sinh y} \, e^{-d/z_0}$$

$$\equiv \exp - \left(\frac{\sinh y_c}{\sinh y} + \frac{1}{\lambda} \right) , \qquad (13)$$

where $\sinh y_c \equiv d/\tau_0$, and $\lambda \equiv z_0/d$ is the "mean induced maturity path" in units of the internucleon distance. In our model, $\tau_0 = 1/m_\pi$ or $y_c = 1.1$ (our results are somewhat insensitive to the precise value for this number), and λ is the model's only free parameter.

We next introduce a propagating matrix G such that after the $k + 1$ collision the distributions are given by

$$\begin{pmatrix} N_{k+1} \\ M_{k+1} \end{pmatrix} = G \begin{pmatrix} N_k \\ M_k \end{pmatrix} . \qquad (14)$$

In terms of the elements of G we have

$$N_{k+1}(i) = G_{NN}(i,j) N_k(j) + G_{NM}(i,j) M_k(j) ,$$
$$M_{k+1}(i) = G_{MN}(i,j) N_k(j) + G_{MM}(i,j) M_k(j) . \qquad (15)$$

For instance, the element $G_{MM}(i,j)$ gives the meson-cluster spectrum at rapidity y_i for *one* incident meson cluster at rapidity y_j.

From the definitions of the inclusive spectra, the inelastic-collision probability, and the immaturity probability, one arrives at the following expressions for the matrix elements of G:

$$G_{NN}(i,j) = V_N(i,j) P_N(1 - Q_j) + \delta_{ij}[1 - P_N(1 - Q_j)] ,$$

$$G_{NM}(i,j) = V_N^L(i,j) P_M(1 - Q_j) ,$$

$$G_{MN}(i,j) = V_M(i,j) P_N(1 - Q_j) , \qquad (16)$$

$$G_{MM}(i,j) = [V_M(i,j) + V_N^R(i,j)] P_M(1 - Q_j)$$
$$+ \delta_{ij}[1 - P_M(1 - Q_j)] ,$$

where the term $V_N^R(i,j)$ in the last equation of (16) comes from assuming that the outgoing-projectile spectrum for an incident meson cluster is the same as that for an incident nucleon. In our calculation, for definiteness, we set $P_M = P_\pi$ (varying P_M would change λ somewhat), which is given in Eq. (12b). From Eq. (16) we see that the immaturity factor Q_j has the net effect of decreasing the internal (other than for the first collision) inelastic-collision probability from the external value of $P_{N(M)}$ to $P_{N(M)}(1 - Q_j)$.

Therefore, Eqs. (7), (8), (9), (12), (13), (15), and (16) allow one to calculate $N_k(i)$ and $M_k(i)$ for any k in terms of only one free parameter λ. For nonintegral k, we make a linear extrapolation. Since the data of Ref. 2 are normalized to inelastic events, one should renormalize the output spectra N_k and M_k by dividing by the inelastic probability factor $1 - (1 - P_N)[1 - P_N(1 - Q_I)]^{k-1}$. The

final-π spectrum is of course obtained from the final-meson-cluster spectrum by allowing each cluster to decay to three pions, as assumed earlier.

As for π-A collisions, the only change from p-A collisions is to replace P_N by P_π, together with the obvious reinterpretation of some symbols due to the change of projectile. Because $P_\pi < P_N$, we expect a smaller number of produced secondaries.

We are now in the position to calculate $\sigma_{\text{inel}}^{pA}$ and $\sigma_{\text{inel}}^{\pi A}$. Within the disk approximation, at a fixed impact parameter b,

$$\sigma_{\text{inel}}^{pA}(b) \propto 1 - S^2 = 1 - (S_1 S_2 \cdots S_{\overline{K}})^2$$
$$= 1 - (1 - P_N)[1 - P_N(1 - Q_I)]^{\overline{K}-1} .$$

Integrating over the transverse area of the nucleus, one gets

$$\sigma_{\text{inel}}^{pA} = C_p A^{2/3} \{ 1 - (1 - P_N)[1 - P_N(1 - Q_I)]^{\overline{K}-1} \} , \qquad (17a)$$

where C_p is independent of A. One should remember that this formula is only applicable for large A. Similarly, one derives

$$\sigma_{\text{inel}}^{\pi A} = C_\pi A^{2/3} \{ 1 - (1 - P_\pi)[1 - P_\pi(1 - Q_I)]^{\overline{K}-1} \} . \qquad (17b)$$

From Eq. (17) one sees that the A dependences of $\sigma_{\text{inel}}^{pA}$ and $\sigma_{\text{inel}}^{\pi A}$ also only depend on the single parameter λ appearing in Q_I. The absolute normalizations of $\sigma_{\text{inel}}^{pA}$ and $\sigma_{\text{inel}}^{\pi A}$ of course depend on C_p and C_π.

III. QUANTITATIVE COMPARISONS WITH DATA

As discussed in Sec. II, our model has only one free parameter λ, the mean induced maturity path. Its value is determined to be $\lambda = 2.4$ by normalizing the model calculation to the 200-GeV p-induced data for $\overline{\nu}_p = 4$.[2] The differential distribution at $\overline{\nu}_p = 4$ is then predicted; furthermore, the normalizations as well as the differential distributions at $\overline{\nu}_p = 2$ and 3 are all predicted. These are shown in Fig. 1. We see that the model reproduces the data reasonably well.[18] In particular for large η, $dn_A/d\eta$ has no or little dependence on A; whereas for small η, $dn_A/d\eta$ grows with $\overline{\nu}_p$ with a slope of order unity. The A dependence of the integrated multiplicity R_A is shown in Fig. 2; the prediction is in fairly good agreement with the data. The energy dependence for p-emulsion collision is shown in Fig. 3 (Ref. 19); the model prediction is not inconsistent with the data; more precise data, especially at cosmic-ray energies, are needed. The model's predictions for π-A collisions at 200 GeV are shown in Fig. 4, again reproducing the data[2] reasonably well. In our model, $\overline{K}$ is the
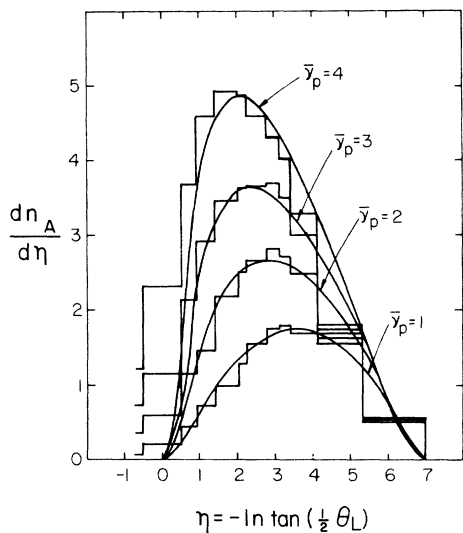
FIG. 1. Variation of $dn_A/d\eta$ as functions of η and $\bar{\nu}_p$ for p-A collision at 200 GeV. Solid lines are our curves; the $\bar{\nu}_p$ =1 curve is the input. Histograms are the data of Ref. 2.
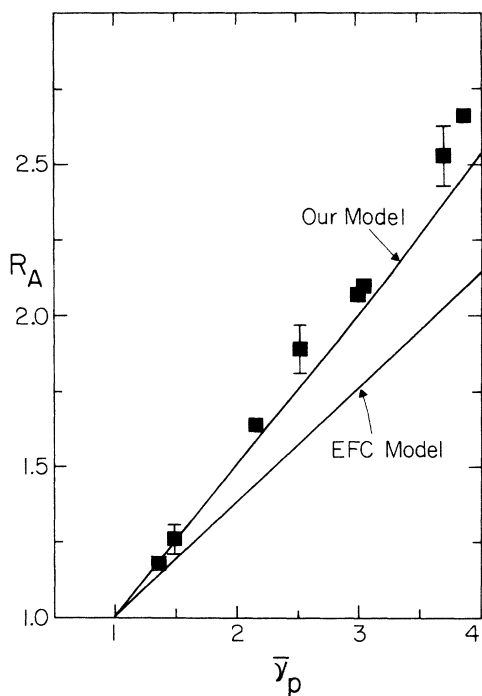

FIG. 2. Variation of the integrated multiplicity R_A with $\bar{\nu}_p$ for p-A collision at 200 GeV. Data points are from Ref. 2; error bars shown represent typical errors of ± 4%. The curve from our model may be parameterized approximately as $R_A \approx 1 + 0.52(\bar{\nu}_p - 1)$. Also shown is the prediction of a refined version (Ref. 1) of K. Gottfried's energy-flux-cascade (EFC) model [Phys. Rev. Lett. 32, 957 (1974)], where $R_A = 1 + 0.38(\bar{\nu}_p - 1)$.
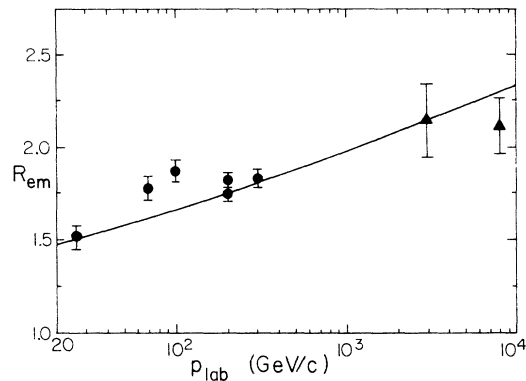

FIG. 3. Variation of R_{emulsion} with incident laboratory momentum p_{lab}. The solid curve is our model prediction. The circle data points are from Ref. 2, and the triangle points are the cosmic-ray data given in Ref. 4 assuming $\sigma_{\text{inel}}^{pN}$ grows like $\ln^2 s$. The p-A data show that the 100-GeV point is higher than the 200-GeV point; however, the π-A data (also of Ref. 2) show that the 100-GeV point is lower than the 200-GeV point.

same for p- or π-induced reactions. It has been pointed out[2] that the experimental pA and πA distributions for identical values of $\bar{\nu}$ have similar behavior. Within our formulation, $\bar{\nu}$ is never introduced. Since we can simultaneously explain both the p-A and π-A data, we feel this coincidence in $\bar{\nu}$ may not have any deep significance. Finally, the A dependences of $\sigma_{\text{inel}}^{pA}$ and $\sigma_{\text{inel}}^{\pi A}$ are
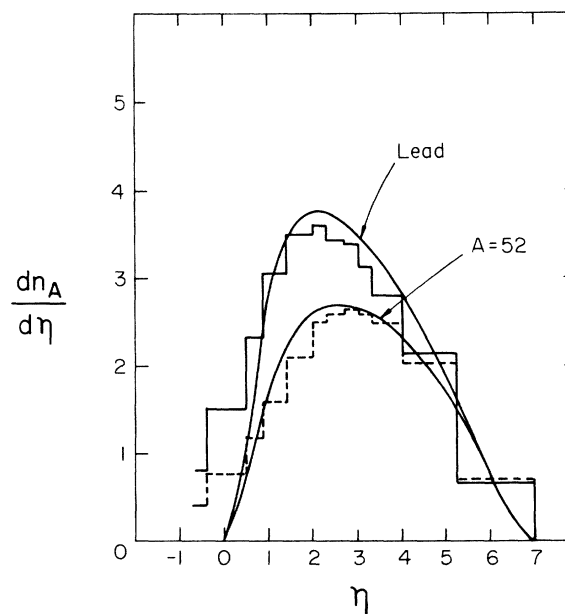

FIG. 4. Variation of $dn_A/d\eta$ for $\pi^- A$ collision at 200 GeV for lead ($\bar{\nu}_\pi = 2.82$, $\bar{K} = 4.7$) and $A = 52$ ($\bar{\nu}_\pi = 2.0$, $\bar{K} = 3.0$). Solid lines are our curves; histograms are the data of Ref. 2.
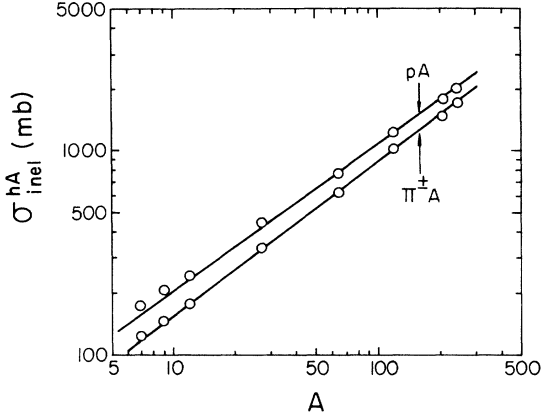
FIG. 5. The A dependence of $\sigma_{\text{inel}}^{pA}$ and $\sigma_{\text{inel}}^{\pi A}$. Solid lines are our curves; the data points are from Ref. 20.

shown in Fig. 5; again the model predictions fit the data[20] well.

We end this section by presenting quantitative calculations of the cut-type model (and without any temporal freezing of degrees of freedom) of Ref. 10 and the fan-plus-cut-type model (and with temporal freezing of degrees of freedom) of Refs. 5-9. We call these model I and model II, respectively.

Model I has no temporal freezing and corresponds to $\tau_0 = 0$ (or $y_c = \infty$). It furthermore neglects the interactions of produced secondaries with subsequent nucleons in the nucleus; this means the internal meson inelastic probability P_M^{int} is set equal to zero. Model I therefore has one free parameter P_N^{int}, the internal nucleon inelastic probability.[21] The predictions of model I with $P_N^{\text{int}} = 0.54$ are shown in Fig. 6; we see that the peaks do not shift enough to the left as A increases and the multiplicities are too large for large η.

In model II, τ_0 is set equal to $1/m$, where m is of the order of m_π. Because it does not have the effect of hadronic enhancement as discussed in Sec. II, it corresponds to $\lambda = \infty$. In its most general form, it allows both the leading particle and the produced secondaries to interact with subsequent nucleons. It therefore has two free parameters, P_M^{int} and P_N^{int}.[22] For $\tau_0 = 1/m_\pi$ (or $y_c = 1.1$), because $Q(y) = \exp(-\sinh y_c/\sinh y) \approx 1$ except for small y, there is essentially no inelastic collision with subsequent nucleons. So even if we give the maximum values to P_M^{int} and P_N^{int}, i.e., $P_M^{\text{int}} = P_N^{\text{int}} = 1$, we still find that R_A are much too small as compared to the data. For $\tau_0 \approx 1/1$ GeV (or $y_c \approx 3$), we can get the right normalization, but the shapes are all wrong because the large-rapidity particles are still suppressed too much from further interacting inelastically. This is shown in Fig. 7 with $P_N^{\text{int}} = 0.60$ and $P_M^{\text{int}} = 0.75$. To fit the data, we find
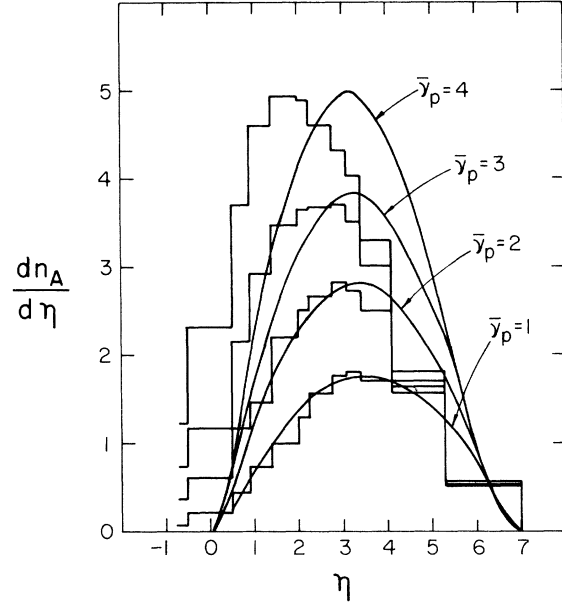

FIG. 6. Predictions of model I (see text) for $dn_A/d\eta$ for p-A collision at 200 GeV.

that we need $\tau_0 \lesssim 1/155\, m_\pi$ (or $y_c \gtrsim 6$); this means that at present energies there is little temporal freezing of degrees of freedom, contrary to the original motivation of the model, and the model now has three free parameters. One could argue that $\tau_0 \sim 1/m$ should be considered in the center-of-mass frame,[23] and not in the rest frame of the particle. The approximate effect of this is to re-
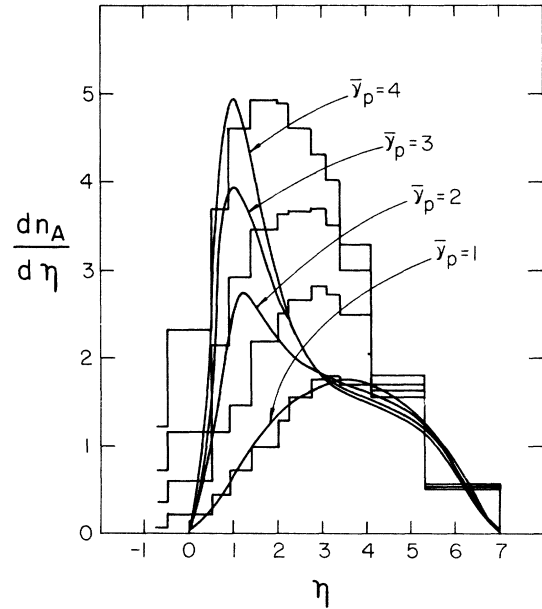

FIG. 7. Predictions of model II (see text) with $\tau_0 \approx 1/1$ GeV for $dn_A/d\eta$ for p-A collisions at 200 GeV.

place $\exp(-\sinh y_c/\sinh y)$ by $\exp[-\sinh y_c/(\sinh y/2)]$; this results in a fit with $\tau_0 \approx 1/1$ GeV (or $y_c \approx 3$). This is a phenomenologically viable model, which is a three-parameter model.

IV. SUMMARY

We have formulated a model based on the iteration of single-particle inclusive distribution. This enables us to take into account some important kinematic effects, but at the same time avoids elaborate Monte Carlo calculation. Within the present formulation, topological multiplicity distribution is not available.

We suggest that at the instant particles are produced during a collision, these particles are very immature, or bare. There is a typical maturity time τ_0, of the order of $1/m_\pi$ in the rest frame of the particle; the presence of other hadronic matter expedites the dressing of the bare particle and so effectively shortens its maturity time. This hadronic enhancement is crucial in explaining the data. The immaturity effect effectively reduces the internal inelastic couplings and so suppresses the overall multiplicity.

The model has only one free parameter λ, the mean induced maturity path. This parameter is fixed by normalizing to the 200-GeV p-A multiplicity data at a fixed A. The parameter-free model then predicts correctly the p-A differential multiplicity as functions of η and A, the multiplicity energy dependence, the π-A differential multiplicity, and the A dependences of σ_{inel}^{pA} and $\sigma_{inel}^{\pi A}$.

We found that the suppression of multiplicity at large y is not only due to a rapidity-dependent suppression factor, but also due to the constraint of energy-momentum conservation in both the secondary cascade and the leading-particle cascade processes.

By explicit quantitative calculations, we have also shown that the so-called fan-plus-cut-type model (with temporal freezing of degrees of freedom)[5-9] and the cut-type model (without temporal freezing of degrees of freedom)[10] are not in agreement with the data.

We suggest that R_A increases very slowly with energy. We also suggest that in comparision to $\overline{\nu}_h$, $\overline{K}$ as defined in the text, especially in the presence of the immaturity effect, is a more model-independent measure of the thickness of the nucleus.

One final word is that because of the immaturity effect and because our model takes into account elastic scattering, the average elasticity of the leading nucleon for h-A collisions is not very much smaller than $\xi \approx 0.5$, the average elasticity of h-h collisions. For example, our calculations for the largest nuclei give $\xi_{hA} \approx 0.35$.

ACKNOWLEDGMENT

*This work was supported in part by the National Science Foundation under Contract No. GR 42060.

†Work supported in part by the Energy Research and Development Administration under Contract No. E(40-1)3992.

[1] For a review, see W. Busza, in *High Energy Physics and Nuclear Structure—1975*, proceedings of the Sixth International Conference, Santa Fe and Los Alamos, edited by D. E. Nagle *et al.* (AIP, New York, 1975).

[2] W. Busza *et al.*, in *Proceedings of the XVIII International Conference on High Energy Physics, Tbilisi, 1976*, edited by N. N. Bogoliubov *et al.* (JINR, Dubna, U.S.S.R., 1977).

[3] For a review, see L. Bertocchi, in *High Energy Physics and Nuclear Structure—1975* (Ref. 1).

[4] For a review of earlier works, see K. Gottfried, in *High Energy Physics and Nuclear Structure—1973*, proceedings of the Fifth International Conference, Uppsala, Sweden, edited by G. Tibell (North-Holland, Amsterdam/American Elsevier, New York, 1974).

[5] O. V. Kancheli, Zh. Eksp. Teor. Fiz. Pis'ma Red. 18, 465 (1973) [JETP Lett. 18, 274 (1974)].

[6] E. S. Lehman and G. A. Winbow, Phys. Rev. D 10, 2962 (1974).

[7] J. Koplik and A. H. Mueller, Phys. Rev. D 12, 3638 (1975).

[8] N. N. Nikolaev, Phys. Lett. 60B, 363 (1976), and references therein.

[9] See also Ref. 3.

[10] A. Capella and A. Kaidalov, Nucl. Phys. B111, 477 (1976).

[11] A condensed version of this work by the same authors was published in Phys. Lett. 68B, 451 (1977).

[12] For definiteness we use $r_A = 1.1A^{1/3}$ fm and $r_N = 1.0$ fm; the latter number is derived from $r_N^{rms} = 0.8$ fm under the uniform density approximation. The precise values used are not important; changing these values slightly has the net effect of slightly changing the only free parameter of the model. See, e.g., A. de-Shalit and H. Feshbach, *Theoretical Nuclear Physics, Vol. 1: Nuclear Structure* (Wiley, New York, 1974); and M. A. Preston, *Physics of the Nucleus* (Addison-Wesley, Reading, Mass., 1962). We thank Dr. K.-K. Kan for discussion on this point.

[13] C. B. Chiu and E. Ugaz, Nucl. Phys. B86, 153 (1975).

[14] Even after including a 10% kaon contribution, the normalization of the p-N data of Ref. 2 seems to be approximately 20% higher than the 205-GeV data of

Y. Cho *et al*., Phys. Rev. Lett. 31, 413 (1973). To be consistent, we use the data of Ref. 2.

[15]See, e.g., M. E. Law *et al*., Lawrence Berkeley Laboratory Report No. LBL-80, 1972 (unpublished).

[16]In case of a black disk, $S = 0$, $P_N = 1$. This means that at each fixed b within the disk there is a complete destructive interference between forward elastic scattering and through-going waves, resulting in the usual black-disk result $\sigma_{el} = \sigma_{inel}$.

[17]D. Bogert *et al*., Phys. Rev. Lett. 31, 1271 (1973).

[18]One should not put too much emphasis on the bins $-1 \leq \eta \leq 0.5$, because our input meson-cluster distribution $V_M(y)$ was constrained to vanish at $y = 0$ and we did not allow the pions to move into the negative-y region as they should. Technically speaking, a proper description of particles near $\eta = 0$ is a very involved task. In additon to pushing the pion distribution to the negative-y region, one needs to correct for the experimental cutoff on the low-momentum events where a detailed specification of transverse momenta is needed.

The effect of Fermi motion of the nucleons is also not negligible in this region.

[19]The data at laboratory energies are compiled in Ref. 2, and the two cosmic-ray data points are from Ref. 4 under the assumption that $\sigma_{inel}^{pN} \sim \ln^2 s$. A word of caution for comparing emulsion data is that different emulsion experiments may have slightly different average A.

[20]For $\pi^- A$ data, see J. C. Allaby *et al*., Sov. J. Nucl. Phys. 13, 295 (1971); W. Busza *et al*., Phys. Rev. Lett. 34, 836 (1975). For $\pi^+ A$ and pA data, see S. P. Denisov *et al*., Nucl. Phys. B61, 62 (1973). The $\pi^+ A$ and $\pi^- A$ cross sections are the same within experimental errors.

[21]In this model one does not have a good physical explanation for the value chosen for the internal coupling P_N^{int}.

[22]This model also does not provide a good physical explanation for the value chosen for the internal couplings P_N^{int} and P_M^{int}.

[23]This idea has also been proposed in Ref. 4.